



21 **ABSTRACT**

22 The sulfur cycle is very important in lake sediments, despite the much lower sulfate
23 concentrations in freshwater than seawater. To date, little is known about the formation and
24 preservation of organic and inorganic sulfur compounds in such sediments, especially in the
25 sulfate-depleted subsurface. Here we investigated the fate of buried S-compounds down to 10-
26 m sediment depth, which represents the entire ~13.5 kya sedimentary history, of the sulfate-
27 rich alpine Lake Cadagno. Chemical profiles of sulfate and reduced sulfur reveal that sulfate
28 from lake water is depleted at the sediment surface with the concomitant formation of iron
29 sulfide minerals. An underlying aquifer provides a second source of sulfate and other oxidants
30 to the deepest and oldest sediment layers generating an inverse redox gradient with ongoing
31 sulfate consumption. Active sulfur cycling within this deep layer produces highly ³⁴S-depleted
32 chromium-reducible sulfur (CRS) ($\delta^{34}\text{S}$ between -45 and -26 ‰ VCDT) and humic-bound
33 sulfur compared to sulfate in lake (+24 ‰) or aquifer water (+12 to +15 ‰) or CRS in surface
34 sediments (-12 to + 13 ‰). Overall, very similar $\epsilon_{\text{sulfate-pyrite}}$ isotope differences in both surface
35 and deep sediments suggest rather comparable closed-system sulfur cycling despite the large
36 differences in sulfate concentrations, organic matter content, and microbial community
37 composition. Although sulfate is depleted in the central part of the sediment column, *dsrB* gene
38 libraries suggest potential for microbial sulfur reduction throughout the sediment column, with
39 sequences in sulfate-depleted layers being dominated by Chloroflexota. Collectively, our data
40 suggest an active sulfur cycle that is driven by uncultivated microorganisms in deep sulfate-
41 depleted sediments of Lake Cadagno.

42

43



44 1. INTRODUCTION

45 The biological sulfur cycle exerts an important control on organic matter burial and thus plays
46 a major role in the global cycling of carbon, oxygen, nitrogen and iron. In anoxic marine
47 sediments, microbial reduction of sulfate (SO_4^{2-}) to hydrogen sulfide ($\Sigma\text{H}_2\text{S}$) is quantitatively
48 the most important respiration reaction, remineralizing upwards of 30% of the total organic
49 carbon flux to the seafloor (Jørgensen, 1982; Bowles et al., 2014; Balzoza et al., 2022). Even in
50 freshwater systems, where sulfate concentrations are typically 100-1,000 times lower than in
51 seawater, high rates of microbial sulfate reduction can be sustained by rapid reoxidation of
52 $\Sigma\text{H}_2\text{S}$ by Fe^{III} , Mn^{IV} , and possibly by redox-active organic substances, e.g. certain humic acids
53 (Pester et al., 2012).

54 Sulfur isotopic fractionation provides important insights into microbial sulfur cycling in
55 the past and present by recording signatures of these processes within different sulfur pools,
56 including sulfide minerals. The preferential reduction of ^{32}S - over ^{34}S -sulfate generates isotopic
57 fractionations of 3 to 75 ‰ between sulfate and hydrogen sulfide in microbial cultures (e.g.
58 (Habicht and Canfield, 1997; Detmers et al., 2001; Brunner and Bernasconi, 2005a; Sim et al.,
59 2011; Bradley et al., 2016)). Nonetheless, the dynamics and controls on the magnitude of sulfur
60 isotope fractionation by sulfate reducing microorganisms have proven to be complex to
61 understand in the environment. While pyrite $\delta^{34}\text{S}$ values supposedly record the S isotopic
62 composition of sulfide in porewater fluids, major isotopic differences (between 10 and 40‰)
63 have been observed between coexisting sedimentary pyrite and dissolved H_2S (Chanton et al.,
64 1987; Canfield et al., 1992; Brüchert and Pratt, 1996; Raven et al., 2016; Lin et al., 2016). These
65 discrepancies have been explained by processes such as sediment remobilization, bioturbation,
66 or post-depositional sediment-fluid interactions (Fike et al., 2015). Recent work of Bryant et al.
67 (2023) indicates that $\delta^{34}\text{S}$ -isotopic variations in marine sediments are largely controlled by



68 physical factors, such as sedimentation rate, along with the supply of Fe and OM. In open
69 systems, the sulfate pool is constantly replenished with light ^{32}S -sulfate, whereas under
70 conditions of rapid sedimentation, sulfate in sediment pore spaces is sealed off from overlying
71 waters and the sulfate pool undergoes Rayleigh distillation. Closed versus open system sulfate
72 reduction can thus explain the large variability in observed fractionations between sulfide and
73 sulfate, which is recorded in sediments by authigenic pyrite.

74 While pyrite is the dominant S pool in most marine sediments, the biggest S pool in
75 many freshwater sediments is organic S (Mitchell et al., 1981; Nriagu and Soon, 1985; Urban
76 et al., 1999). This organic S originates from both the settling of seston material and the microbial
77 reduction of water column-derived sulfate to hydrogen sulfide, which then reacts with
78 sedimentary organic matter (David and Mitchell, 1985; Rudd et al., 1986). The sulfurization of
79 organic matter tends to promote organic matter resistance to microbial degradation and is thus
80 believed to contribute significantly to long-term preservation of organic carbon in sediments
81 (Damsté and De Leeuw, 1990; Hebbing et al., 2006), and to petroleum formation (Orr and
82 Damsté, 1990). Though it is likely that some microorganisms are capable of degrading fractions
83 of this organic S pool, their activity and identity is unknown.

84 Recently, the metabolic capacity for sulfur cycling has been expanded to new
85 phylogenetic groups based on the detection of specific marker genes for sulfur cycling within
86 these taxa (e.g., Anantharaman et al., 2018). Although the presence of such genes must be
87 interpreted with caution, their distribution across environments can help illuminate the
88 distributions of putative sulfur reducing and sulfur oxidizing microbial communities.
89 Thiosulfohydrolase of the sulfur oxidation (Sox) enzyme system (*soxB*) is one such marker
90 gene and has been widely employed to characterize the diversity of sulfur-oxidizing bacteria
91 (SOB) (Meyer et al., 2007). Another example is dissimilatory sulfite reductase (*dsrAB*), an



92 enzyme that catalyzes the reduction of sulfite to sulfide and is used by all known sulfate
93 reducers (Klein et al., 2001).

94 Because low rates of microbial sulfur cycling continue in sulfate-depleted marine
95 sediments (Holmkvist et al., 2011; Treude et al., 2014; Brunner et al., 2016; Pellerin et al.,
96 2018a), such processes may likewise occur in sulfate-depleted sediments of lakes and leave a
97 lasting imprint on the lake sulfur geochemical record. Here we investigate the potential for
98 microbial sulfur cycling in Lake Cadagno, which is an intermediate system between freshwater
99 and seawater, due to its elevated sulfate concentrations (1-2 mM). We combine chemical and
100 isotopic analyses of major S and C phases with quantification and sequencing of S-cycling
101 genes (*dsrB*, *soxB*) to investigate S cycling across the complete ~13.5 kya sedimentary history
102 of Lake Cadagno.

103 **METHODS**

104 ***1.1 Geological setting***

105 The meromictic Lake Cadagno, located in the Swiss Alps, contains 1-2 mM dissolved sulfate,
106 which originates from the dissolution of sulfate-bearing dolomite bedrock via subaquatic
107 springs. Since its formation ~13.5 kya, Lake Cadagno has undergone a complex redox history,
108 transitioning from seasonal stratification around 12.5 kya to complete euxinia about 10.9 kya
109 (Wirth et al., 2013; Berg et al., 2022). Preliminary analyses of sulfur phases in surface and deep
110 sediments (Berg et al., 2022) reveal two sulfate depletion zones (SDZ).

111 All Lake Cadagno deep sediment core sampling, geochemical analyses of sediment and
112 porewater, and DNA extractions were performed as described in (Berg et al., 2022). Additional
113 samples for sulfate isotope analyses were obtained in June 2020 from one surface spring (at



114 SwissGrid coordinates 2'697'763, 1'155'959) and one subaquatic spring at approximately 5 m
115 depth (2'697'521, 1'156'044) located on the south side of the lake.

116 ***2.2 Solid-phase sulfur extractions***

117 Sequential sulfur extractions were performed based on the protocol of Ferdelman et al. (1991).
118 First, elemental sulfur was extracted under N₂ atmosphere three times with degassed 100%
119 methanol. During each step the methanol-sample mixture was sonicated for 10 min in an ice
120 bath, centrifuged, and then the methanol was pipetted into a clean vial. Methanol extracts were
121 analyzed by ultrahigh pressure liquid chromatography (UPLC) using a Waters Acquity H-class
122 instrument with an Acquity UPLC BEH C18, 1.7 μm, 2.1 × 50 mm column (Waters, Japan) and
123 a PDA detector (absorbance wavelength set to 265 nm). The injection volume was 10 μl with
124 methanol as eluent flowing at 0.2 ml min⁻¹. Elemental sulfur eluted at 4.14 min.

125 Next, humic acids were extracted 3 times, or until the supernatant was clear, with
126 degassed 0.1 M NaOH and collected in 50 ml Falcon tubes. Silicates were precipitated from the
127 base extracts by addition of saturated NaCl solution (5 mL per 45 mL extract) and removed by
128 centrifugation and decanting. The basic extract was acidified to pH 1.5 with concentrated HCl,
129 allowed to stand at 4°C overnight, and centrifuged to precipitate humic acids. These were
130 washed three times with distilled water to remove salts prior to drying and C, N, and S analysis.

131 Finally, acid-volatile sulfur (AVS) and chromium-reducible sulfur (CRS) were
132 extracted from the remaining sediment using the two-step acid Cr-II method (Fossing and
133 Jørgensen, 1989; Kallmeyer et al., 2004). For the AVS fraction, 6 N HCl was added to sediment
134 in a reaction flask under an N₂ atmosphere and H₂S was trapped by bubbling through a 5% Zn-
135 acetate solution for 2 h. The CRS fraction was subsequently obtained by adding 20 ml of the
136 organic solvent dimethyl sulfoxide and 16 ml of CrCl₂ solution and reacting again for 2 h. AVS



137 and CRS fractions, collected as ZnS, were quantified photometrically as above, pelleted by
138 centrifugation, rinsed with MilliQ, and dried at 50°C prior to $\delta^{34}\text{S}$ analyses as described below.

139 Isotopic compositions of sulfur in the sedimentary AVS, CRS and humic acid sulfur
140 (HAS) fractions, and of dissolved sulfate from sediment porewater, a subaquatic spring, and
141 two surface springs, were determined using a Flash-EA 1112 (ThermoFisher) coupled to an
142 isotope ratio mass spectrometer (IRMS, Delta V, ThermoFisher) by addition of vanadium
143 pentoxide as a catalyst. Isotope ratios are reported in the conventional δ -notation with respect
144 to the Vienna-Cañon Diabolo Troilite (VCDT) standard for sulfur. The system was calibrated
145 for sulfur using the international standards for sulfide and sulfate: IAEA-S1 ($\delta^{34}\text{S} = -0.3\text{‰}$),
146 IAEA-S2 ($\delta^{34}\text{S} = +22.67\text{‰}$), IAEA-S3 ($\delta^{34}\text{S} = -32.55\text{‰}$) and IAEA-SO5 ($\delta^{34}\text{S} = +0.49\text{‰}$),
147 IAEA-SO6 ($\delta^{34}\text{S} = -34.05\text{‰}$), NBS-127 ($\delta^{34}\text{S} = +21.1\text{‰}$), respectively. Reproducibility of the
148 measurements was better than 0.2‰. This method also produced the weight % sulfur in the
149 humic acid extracts.

150 Total sulfur (TS) was determined together with total carbon (TC) and total organic
151 carbon (TOC) on bulk, freeze-dried sediments as described in (Berg et al., 2022) and TIC was
152 calculated as the difference between TC and TOC.

153 ***2.3 DNA extraction and sulfur-cycling gene analyses***

154 DNA was extracted from frozen sediment according to the lysis protocol II of (Lever et al.,
155 2015) as outlined in (Berg et al., 2022). The *dsrB* gene was PCR-amplified using the *dsrB* F1a-
156 h / 4RSI1a-f primer mixtures from (Lever et al., 2013). *soxB* genes were amplified using the
157 recently designed *soxB*-837F1a-l / *soxB*_1170R1a-g primer mixtures (Deng et al., 2022).
158 Quantitative PCRs (qPCR) were performed on a LightCycler 480 II system using the reagent
159 mixtures outlined in (Jochum et al., 2017). The thermal cycler settings were (1) enzyme
160 activation and initial denaturation at 95°C for 5 min; (2) 60 cycles of (a) denaturation at 95°C



161 for 30 s, (b) annealing at 56°C (*dsrB*) or 60°C (*soxB*) for 30 s, (c) elongation at 72°C for 25 s,
162 and (d) fluorescence acquisition at 82°C (*dsrB*) or 86°C (*soxB*) for 5 s; and (3) a stepwise
163 melting curve from 60 to 95°C to check for primer specificity. Plasmids containing full-length
164 *dsrAB* and *soxB* genes of *Desulfotomaculum carboxydivorans* and *Thiobacillus denitrificans*,
165 respectively, were applied as qPCR standards.

166 *dsrB* gene sequences were phylogenetically annotated using the ARB software
167 (www.arb-home.net) based on an updated version of the *dsrAB* database published in (Müller
168 et al., 2015). This database was expanded by adding *dsrAB* gene sequences from since then
169 published metagenomes, as well as closest BLAST hit to *dsrB* gene sequences detected in Lake
170 Cadagno. The phylogenetic annotation was based on a *dsrAB* gene bootstrap tree that was built
171 by ARB Neighbor-Joining with Jukes-Cantor correction using diverse *dsrAB* reads that covered
172 the entire *dsrB* gene amplicon sequence and were at least 750 bp in length. The shorter amplicon
173 sequences from Lake Cadagno, as well as closest BLAST hits that were <750 bp long, were
174 added using the ARB Parsimony option combined with a newly designed, amplicon-specific
175 *dsrB* filter that removed hypervariable regions.

176 2. RESULTS

177 2.1 Sulfur Geochemistry in Lake Cadagno sediments

178 The complete sedimentary sequence from Lake Cadagno is approximately 950 cm long,
179 covering a period of ~13.5 ky (Berg et al., 2022). Sediments are characterized by relatively fine
180 grained pelagic lacustrine sediments intercalated with frequent coarser-grained flood- and mass
181 movement-derived deposits containing remobilized littoral lake and terrestrial sediment in the
182 upper 790 cm, underlain by light-colored fine-grained deposits of late glacial origin (Fig. 1).
183 The sediment can thus be divided into three distinct lithostratigraphic units representing an early
184 oxic lake (950-790 cm; 13.5 to 12.5 kya), a redox transition interval (790-760 cm; 12.5 to 10.9

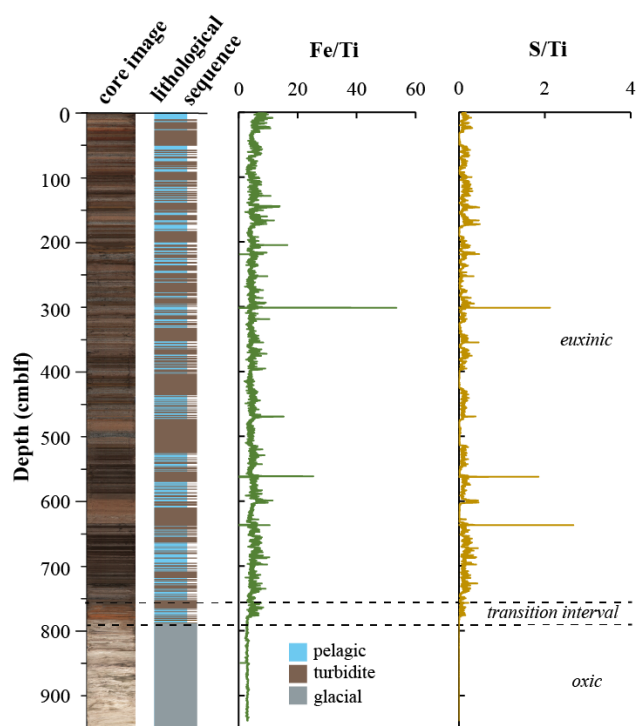


185 kya), and the euxinic period (above 760 cm; 10.9 kya to present). High-resolution mapping of
186 element geochemistry on split core surfaces (Fig. 1) reveals that the accumulation of sulfur is
187 restricted to sediments deposited after the onset of periodic anoxia (transition interval) to
188 permanently reducing conditions (euxinic interval). Fe and S were normalized against Ti, which
189 represents the lithogenic fraction unaltered by redox processes in the aquatic environment. The
190 correlation between S/Ti and Fe/Ti suggests the presence of authigenic iron sulfide phases. The
191 largest S excursions are located at 300, 560, and 637, which correspond to lacustrine deposits
192 according to the lithological
193 sequence.

194 To obtain further
195 insights into sulfur redox
196 cycling in these sediments,
197 major solid sulfur phases
198 were quantified (Fig. 2A).
199 Elemental sulfur (S^0) is the
200 most abundant solid sulfur
201 phase in surface sediments at
202 300 $\mu\text{mol/g}$ dry sediment.
203 The parallel decrease in S^0
204 and Fe^{III} with depth indicate
205 increasingly reducing
206 conditions. Both AVS

207 (mostly amorphous FeS and mackinawite) and HAS exhibit a peak at 10 cm depth, and then
208 decrease in parallel with S^0 at the expense of CRS formation. In sediments below 20 cm, S^0 and
209 AVS are barely or not detectable whereas HAS concentrations are relatively constant (0.42 -

Figure 1 | Lithological profile determined from a composite core image of the sedimentary sequence retrieved from Lake Cadagno. XRF profiles of S/Ti and Fe/Ti. Changes in lake redox chemistry are denoted by dashed lines.



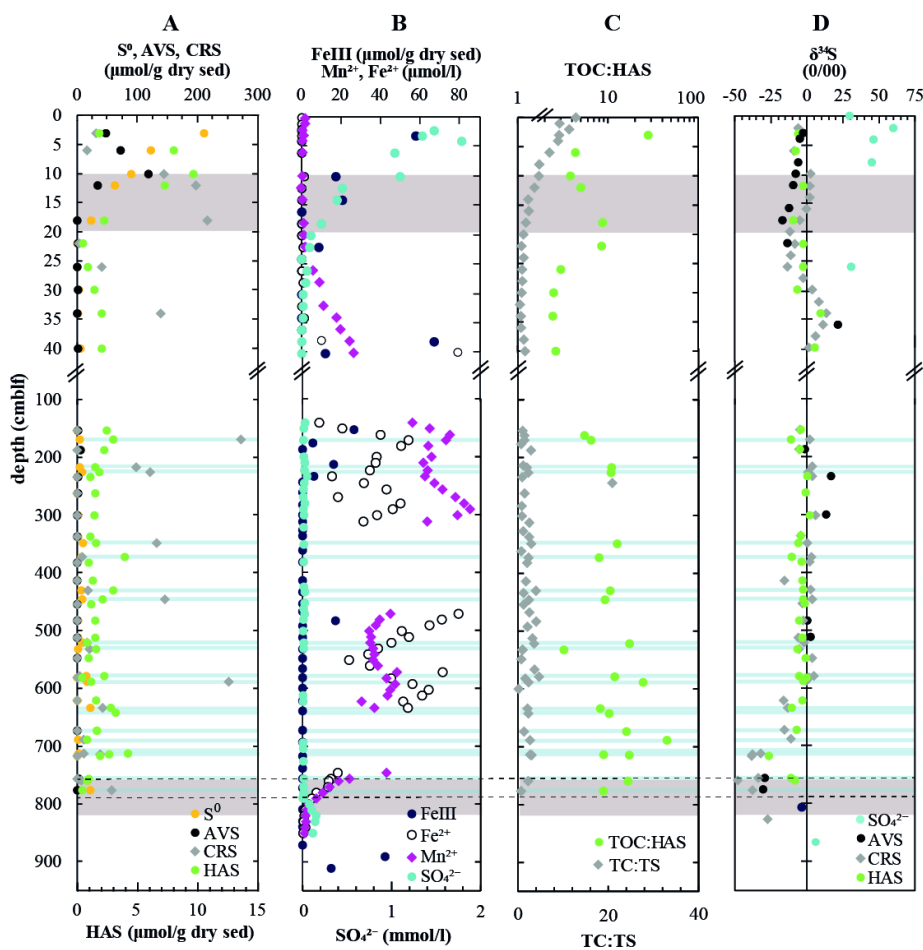


Figure 2 | Geochemistry of major solid-phase sulfur pools (A) along with metals and dissolved species (B) involved in sulfur cycling in the sediment column of Lake Cadagno. (C) Ratios of total and organic carbon to sulfur and humic-acid bound S, respectively, along with (D) isotope ratios of major sulfur pools. Based on previous analyses (Berg et al 2022), the sulfate depletion zones have been shaded in gray and lacustrine deposits have been shaded in blue. Note the break in the y-axis.

210 4.40 $\mu\text{mol/g dry sed}$) and CRS levels fluctuate widely (0-270 $\mu\text{mol/g dry sed}$). The highest
 211 concentrations of CRS and HAS are associated with lacustrine deposits. In the deep euxinic
 212 sediments exceptionally high CRS contents were detected in a handful of samples that are
 213 typically lacustrine deposits and follow broadly the same trend as Fe^{2+} concentrations (Fig. 2B).



214 At 760 cm, a second SDZ has been described based on an upwards-diffusing gradient
215 of sulfate thought to originate from a subterranean aquifer (Berg et al., 2022). The change in
216 redox conditions at 775 cm depth is marked by a small peak in AVS (9 $\mu\text{mol/g}$ dry sed) and S^0
217 (23 $\mu\text{mol/g}$ dry sed). In concurrence with extant oxidizing conditions, late glacial sediments
218 below 790 cm are poor in reduced sulfur and organic matter but contain measurable iron oxides
219 and up to 0.2 mmol/l sulfate in porewaters (Fig. 2B). These sulfate concentrations are much
220 lower than concentrations of sulfate in lake bottom water (1.8 mmol/l), but in the same general
221 range as a subaquatic spring (268 $\mu\text{mol/l}$) and a surface spring (166 $\mu\text{mol/l}$).

222 C to S ratios of organic matter are expected to decrease when sulfide reacts with organic
223 matter to form organic S, or when microorganisms preferentially degrade organic carbon and
224 leave behind organic S. TC:TS decreases from 12 at the surface to about 1.3 at 20 cm depth and
225 remains relatively constant throughout the deeper sediments (Fig. 2C). Most of this carbon is
226 in organic form, with measurable contributions of total inorganic carbon (TIC) present only in
227 surface sediment and again at 400 cm depth (<2 wt%; Fig. S1). A part of the total organic sulfur
228 could be measured as HAS, and the ratios of TOC:HAS exhibit a very different behavior (Fig.
229 2C). TOC:HAS was lowest at 25-40 cm depth and the rather high, widely fluctuating values
230 below this depth are mostly due to the low TOC content.

231 Sufficient sulfate for isotopic analyses was only obtained from five surface samples and
232 by pooling porewater from the entire late glacial sediment sequence (790-910 cm). Sulfate in
233 the upper sediments is highly enriched in ^{34}S , increasing from 24 ‰ in the bottom waters to 60
234 ‰ within the upper 2 cm. This zone coincides with strong decreases in TOC and isotopically
235 light ^{13}C -DIC values, which indicate high rates of organic matter mineralization (Berg et al.,
236 2022; Gajendra et al., 2023). $\delta^{34}\text{S}$ -sulfate profiles measured in 1991 exhibit increasing
237 enrichment in ^{34}S down to the SDZ (Fig. S2) with the highest values of approximately 60‰ at
238 10 cm depth, somewhat deeper than at present. In the deep glacial sediments, the sulfate isotopic



239 signature is relatively light (+7‰), which is more similar to values measured in subaquatic
240 (+12‰) and surface (+15‰) springs.

241 Sulfide in Lake Cadagno sediments is generally depleted in ^{34}S relative to sulfate in the
242 overlying water column (Fig. S2). $\delta^{34}\text{S}$ -AVS becomes progressively lighter with depth in
243 surface sediments, decreasing from -2‰ at the lake floor to a minimum value of -16‰ in the
244 upper SDZ, but very little AVS was recovered from the mid-column and deep sediments. For
245 those samples with measureable $\delta^{34}\text{S}$ -AVS, it fluctuates between -9‰ and +17‰ with no
246 discernible trend. In the deep SDZ, $\delta^{34}\text{S}$ -AVS becomes strongly negative, exhibiting values as
247 low as -34‰ coinciding with lighter porewater sulfate (+6.8‰). CRS is more depleted in ^{34}S
248 than AVS in the limited samples available, except for in the upper SDZ where $\delta^{34}\text{S}$ -CRS values
249 are enriched by ~2‰ relative to $\delta^{34}\text{S}$ -AVS. In the deep SDZ, extremely light CRS values are
250 observed down to -47.5‰, which is equivalent to a fractionation of 54‰ compared to deep
251 porewater sulfate. $\delta^{34}\text{S}$ -HAS are consistently heavier than AVS and CRS, varying between 0‰
252 and -26‰ down to 750 cm depth in respective sediment layers. No significant difference in
253 HAS isotopic composition was found between sediment layer types.

254 ***3.2 Genetic potential for microbial sulfur cycling***

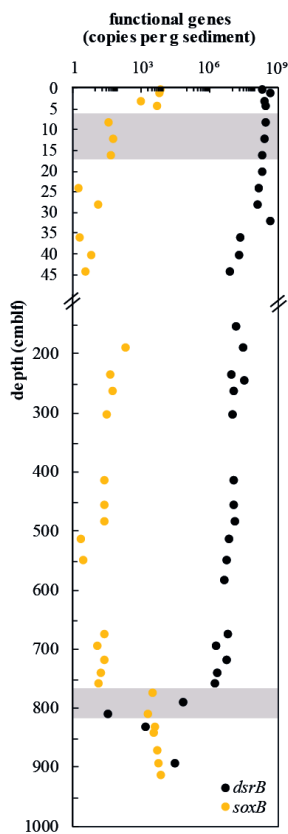
255 Abundances of sulfur-cycling microorganisms in the Lake Cadagno sediment column were
256 assessed by qPCR of functional genes for sulfate reduction (*dsrB*) and sulfur oxidation (*soxB*)
257 (Fig. 3). Copy numbers of *dsrB* gradually decrease from surface sediments (4.23×10^8 copies/g
258 wet sediment) to the upper SDZ (7.17×10^6 copies/g, 44 cm depth). Throughout the SDZ (35
259 cm and below), gene copy numbers remain relatively stable between 1.58×10^6 and 2.9×10^7
260 copies/g wet sediment. Within the lower sulfate-methane depletion zone at around 810 cm
261 depth, *dsrB* copy numbers drop off greatly, to values of 10^1 and 3.10×10^3 and copies/g before



262 increasing again to 2.77×10^4 copies/g in parallel with increasing sulfate concentrations in the
 263 underlying oxic, glacial interval (Fig. 3; also see Fig. 1).

264 Surprisingly, *soxB* was detectable throughout the entire sediment column. Highest
 265 values (up to 6.45×10^3 copies/g sediment) were found in the sulfate-rich surface sediments
 266 down to the SDZ. In mid-column sediments, sulfur oxidation gene copies were much lower
 267 (1.84×10^0 - 1.93×10^2 copies/g) before increasing again in the lower SDZ and reaching a second

Figure 3 Depth profiles of *dsrB* and *soxB* gene copy numbers. Copies of both genes were detectable by qPCR in all samples targeted. Shaded gray regions indicate sulfate-methane depletion zones.



peak in the glacial sediment layer (6.59×10^3 copies/g). This increase in sulfur oxidation potential matches the oxidizing, and most likely oxic, conditions in this deep glacial sediment layer that are by the presence of Fe-oxides, elemental sulfur, and sulfate (Fig. 2A&B). Sulfur oxidizing bacteria appear to make up a large part of the total microbial population in this layer, with an average ratio of *soxB* to 16S DNA copies/g sediment of 1.17 ± 1.34 . At the same time, 16S qPCR data indicate a drop in microbial population size from 10^8 copies/g sediment in the lower SDZ to 10^3 to 10^5 copies/g in the deep glacial layer (Berg et al., 2022).

3.3 Diversity of sulfate-reducing microorganisms

Sequencing of the sulfate reduction gene (*dsrB*) revealed a diverse assembly of potential sulfate reducers in Lake Cadagno sediments (Fig. 4). The majority of sequences could not be classified beyond the supergroup level, indicating that they belong to novel lineages. Overall, the sulfate reducers identified in our gene amplicon libraries



286 were consistent with those identified in 16S rRNA gene libraries, with high relative abundances
 287 of Deltaproteobacteria, Nitrospirae, and Chloroflexota (Berg et al., 2022). The community
 288 profile shows a clear differentiation between surface sediment and deeper sulfate-depleted
 289 layers, and there is a clear decrease in taxonomic diversity with depth and sediment age.

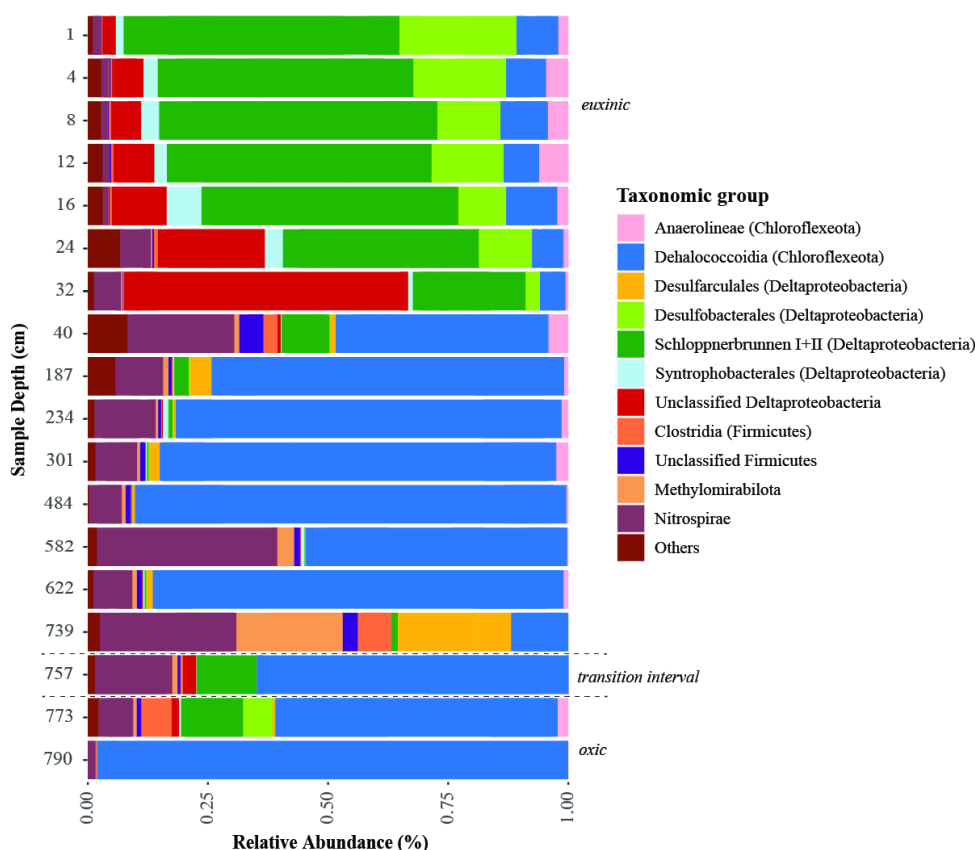


Figure 4 | Taxonomic classification of functional genes *dsrB* recovered from the Lake Cadagno sediment depth. Sediment geological transitions are indicated with dashed lines.

290 Similar to other sulfate-rich sedimentary environments, Lake Cadagno surface
 291 sediments harbor highly abundant (>80% relative abundance) Desulfobacterota (formerly
 292 Deltaproteobacteria). Most of these belong to uncultured members of the order
 293 Desulfobacterales, clade Schloppnerbrunnen I + II (originally identified in peatland soils), and
 294 other unclassified Deltaproteobacteria. In addition, reads belonging to the genus *Desulfomonile*,



295 of which members are known to also disproportionate sulfur intermediates (Slobodkin and
296 Slobodkina, 2019), are well represented in sediments between 4 cm and 28 cm below the
297 sediment surface (2%-8% of the total community).

298 Below the SDZ at 40 cm there is a shift in the sulfate-reducing microbial assemblage
299 toward the dominance of uncultivated Chloroflexota. Members of this phylum have so far not
300 been demonstrated to perform dissimilatory sulfur cycling but Chloroflexota *dsrB* sequences
301 have been found in deep sedimentary marine environments (e.g. Vuillemin et al., 2020; Liu et
302 al., 2022). A second compositional shift occurs in deeper layers around the redox transition
303 interval at 739 cm depth. Genes for sulfate reduction in these layers affiliate with Clostridiales,
304 Dehalococcoidia, Methylospirales, and the phylum Nitrospirae. Sulfate reducers belonging
305 to Desulfobacterota also reappear close to the redox transition but are distinct from those in
306 surface sediments, affiliating mostly with the species *Desulfoarculus baarsii* (classified within
307 the order Desulfarculales). In the deep glacial sediment (> 790 cm), the diversity of microbial
308 sulfate-reducers is reduced (98% of *dsrB* sequence reads) to Chloroflexota from the classes
309 Anaerolineae and Dehalococcoidia.

310 3. DISCUSSION

311 4.1 Evidence for continued sulfur cycling in sulfate-depleted sediments

312 The relatively heavy isotopic signature of sulfate in Lake Cadagno bottom waters ($\delta^{34}\text{S} = +24$
313 ‰) compared to the $\delta^{34}\text{S}$ of source waters observed in subaquatic +12‰ and surface springs
314 +15‰ indicate active sulfate reduction in the anoxic lower part of the water column. These
315 values are consistent with previously measured values of surface (+12‰) and bottom water
316 (+30‰) sulfate (Canfield et al., 2010). The $\delta^{34}\text{S}$ values of sulfate in the Lake Cadagno springs
317 are the same as those of other springs in the Valle Leventina (Steingruber et al., 2020) indicating



318 dissolution of gypsum/dolomite in the marine evaporites from the Middle Triassic ($\delta^{34}\text{S}$ circa
319 +15‰) as the main source (Bernasconi et al., 2017).

320 Microbial sulfur cycling in the sulfate-rich uppermost sediment layer (0-24 cm) appears
321 to be primarily driven by Desulfobacterota. Below this depth, mostly uncultured groups of
322 unclassified Deltaproteobacteria and Dehalococcoida possess an unexplored genetic potential
323 for sulfate reduction. The high input of labile, microbial organic carbon from the overlying
324 water column supports very high rates of anaerobic organic carbon mineralization within the
325 upper 20 cm (Gajendra et al., 2023). As a result, TOC drops from 15-20 wt. % at the lake floor
326 to values of ≤ 5 wt. % below 20 cm. Microbial sulfate reduction appears to be primarily linked
327 to the degradation of this organic matter (Berg et al., 2022) though sulfate-driven AOM may
328 additionally occur within the top 2-3 cm (Schubert et al., 2011). Vertical shifts in dominant S-
329 cycling microorganisms from surface sediments (Schloppnerbrunnen I + II, Desulfobacterales
330 (all Desulfobacterota) to Unclassified Desulfobacterota in deeper layers suggest a key influence
331 of sulfate concentrations and organic matter quality on sulfate-reducing microbial community
332 structure. Herein Desulfobacterales include several known sulfate-reducing and sulfur-
333 disproportionating genera, such as *Desulfobulbus*, *Desulfovibrio*, and *Desulfomonile* (Cypionka
334 et al., 1998; Wasmund et al., 2017; Hashimoto et al., 2022). Similar shifts in dominant sulfate-
335 reducing communities from significant abundances of known groups with cultured
336 representatives in surface layers to dominance of physiologically unclassified taxa in deeper
337 layers have been reported from marine sediments (Jochum et al., 2017). We also detected genes
338 for sulfur oxidation, despite the anoxic nature of these sediments.

339 As sulfate concentrations drop below detection below 30 cm depth, there is a clear shift
340 in dominance from Desulfobacterota to Chloroflexota (Fig. 4). Nevertheless, *dsrB* gene
341 abundances remain high suggesting that sulfate/sulfur reduction likely continues in sulfate-
342 depleted sediments parallel to fermentation and methanogenic metabolisms. It is possible that



343 sulfate or other oxidized sulfur species, that are regenerated by sulfur oxidation reactions with
344 metal oxides, support these communities of S-cycling microorganisms. Alternatively, the high
345 abundances of Chloroflexota from the class Dehalococcoidia could suggest alternative sulfur-
346 based metabolic activities. Several studies have proposed Chloroflexota to be involved in the
347 metabolism of organic sulfur compounds (Wasmund et al., 2014; Mehrshad et al., 2018), with
348 genomic analyses from deep sea sediments indicating genetic potential for dimethylsulfide,
349 methane sulfonate, and alkane sulfonate metabolisms (Liu et al., 2022). Overall, our findings
350 are consistent with studies of marine sediments demonstrating active sulfate reduction below
351 the zone of sulfate depletion (Holmkvist et al., 2011; Treude et al., 2014; Brunner et al., 2016;
352 Pellerin et al., 2018b) and suggest that deep sulfate reduction also can occur in lake sediments.

353 An oxidizing front and constant groundwater supply of sulfate at the transition between
354 euxinic and deep glacial deposits appears to sustain continuous microbial sulfur cycling at 760-
355 800 cm depth. Opposite trends of *dsrB* and *soxB* gene copies reveal a physical separation
356 between S reduction and oxidation in this layer indicating a switch from anoxic to oxic
357 conditions. $\delta^{34}\text{S}$ of CRS values that are depleted by -40 and -50 ‰ relative to those of $\delta^{34}\text{S}$ -
358 sulfate suggest the presence of an active sulfur cycle driven by slow diffusion of groundwater
359 sulfate into the deepest layers of lake sediment. Extremely slow sulfate reduction rates tend to
360 generate very light sulfide, especially in a diffusive rather than closed system (Goldhaber and
361 Kaplan, 1980; Habicht and Canfield, 1997; Ono et al., 2014), which is then preserved in the
362 CRS pool over geological time scales. It can also not be ruled out that these low $\delta^{34}\text{S}$ values are
363 due to repeated cycles of reduction and partial re-oxidation of H_2S , e.g. by chemical oxidation
364 to S^0 by iron oxides followed by microbial S disproportionation (Canfield and Thamdrup, 1994)
365 and/or by sulfur reduction (Wortmann et al., 2001; Brunner and Bernasconi, 2005b; Canfield
366 et al., 2010; Sim et al., 2011). Single-step reduction of light S^0 appears to be the more
367 parsimonious scenario as the disproportionation model requires heavy sulfate to be removed



368 from the system to avoid producing heavy sulfide. Nonetheless, iron oxides in the deep glacial
369 layers are likely to oxidize (downward-diffusing) H_2S and may explain the abundant elemental
370 S^0 measured at the deep redox transition.

371 ***4.2 Rapid degradation and sulfurization are controlled by organic matter quality***

372 Major changes in solid-phase sulfur pools occur within the upper 20 cm of sediment
373 corresponding to the very high rates of organic matter degradation and microbial sulfate
374 reduction (Berg et al., 2022). These changes include a shift from elemental S and AVS as the
375 dominant S pools at 0-10 cm to CRS (which contains pyrite) as the main S pool between 10-20
376 cm. This CRS likely derives from chemical reactions of AVS (containing FeS) and elemental
377 sulfur (including polysulfides) (Luther, 1991). Below 20 cm, CRS remains the dominant S pool,
378 and moreover, shows a highly significant ($p < 0.001$) enrichment in lacustrine layers versus
379 mass-movement deposits. The elevated CRS in lacustrine layers confirms the notion that most
380 iron sulfides are of authigenic (rather than terrestrial) origin and result from anaerobic
381 breakdown of lacustrine organic matter driving sulfate reduction. In addition to CRS formation,
382 we observe the sulfurization of organic matter in these (<100-year-old) surface sediments, as
383 indicated by the strong increase in HAS in the top 0-10 cm. This observation is consistent with
384 studies on several other lakes in Switzerland, which reported that most organic matter
385 sulfurization occurs within the initial decades after sediment deposition (Urban et al., 1999;
386 Hebting et al., 2006).

387 The observed high rates of organic matter sulfurization in surface sediments suggest that
388 differences in organic matter quality affect organic matter degradation rates and may also affect
389 the incorporation of sulfur into organic matter. Notably, the highest concentrations of HAS
390 were recovered from lacustrine layers. This suggests that fresh lacustrine organic matter from
391 the lake water column is more easily sulfurized than refractory terrestrial organic matter from



392 the lake watershed. While the chemical composition of this sulfurized organic matter remain
393 unclear, it is worth noting that lipid-rich algal and microbial material are rapidly degraded in
394 surface sediments, carbohydrates appear to be selectively preserved, thus increasing in
395 contribution to total organic matter in deeper layers (Gajendra et al., 2023). This effective
396 preservation of carbohydrates could be related to macromolecular matrices that are rich in
397 degradation-resistant structural polymers (e.g. hemicelluloses and pectin in microalgal and
398 terrestrial plant biomass; (Gajendra et al., 2023)). In addition, the high chemical reactivity of
399 carbohydrates with sulfide could play a role. Past research has shown that carbonyl functional
400 groups are more reactive with inorganic sulfur species than hydroxyl groups, explaining why
401 carbohydrates with a carbonyl group in the C₁ position constitute a major part of sulfurized
402 organic matter in marine sediments (Damsté et al., 1998) and in laboratory experiments (Kok
403 et al., 2000). The same could be the case, leading to carbohydrates in deeper sediment layers of
404 Lake Cadagno to be effectively preserved because of sulfurization. Alternatively, it is possible
405 that sulfur that is incorporated into carbohydrates is selectively preserved as organic S because
406 the surrounding carbohydrate matrices are degradation-resistant.

407 Deeply buried organic sulfur in Lake Cadagno is more enriched in $\delta^{34}\text{S}$ than co-
408 occurring pyrite which is consistent with measurements from marine systems (e.g. (Goldhaber
409 and Kaplan, 1980; Anderson and Pratt, 1995; Werne et al., 2003; Raven et al., 2016, 2023)).
410 Humic sulfur consists of sulfoxides or sulfones and, in a more reduced state, organic sulfides
411 and/or organic polysulfides (Ferdelman et al., 1991). These distinct classes of organic S
412 compounds exhibit different ^{34}S isotope signatures (Raven et al., 2015), and may have different
413 source molecules (e.g., sulfate esters) than sulfur that is present in pyrite (e.g., inorganic
414 sulfate). Because the fractionation factor of organic matter sulfurization is almost negligible
415 (Amrani and Aizenshtat, 2004), it is likely that the timing of formation is responsible for HAS
416 being heavier, on average, than CRS which forms first and leaves behind a slightly heavier pool



417 of sulfate/sulfide. Another explanation is that HAS is very stable (as mentioned above) and less
418 likely to be re-oxidized and undergo additional fractionation cycles.

419 ***4.3 Diffusive-dominated sulfate reduction in both surface and deep sediments***

420 Rayleigh distillation exerts a strong control on $\delta^{34}\text{S}$ signatures in sediments where diffusion
421 limitations imply that sulfate cannot be replenished as rapidly as it is removed by microbial
422 reduction and precipitation. For this reason, it has been postulated that at high rates of
423 sedimentation, porewater sulfate is effectively trapped and the system closed off from exchange
424 with the overlying water column (Bryant et al., 2023). The opposite is true for diffusive systems,
425 where a constant supply of sulfate can feed continued production of light sulfide. In Lake
426 Cadagno surface sediments (above the first mass movement deposit at 30 cm), the relatively
427 large differences (44 to 66 ‰) in $\delta^{34}\text{S}$ between sulfate and CRS are in the same range as those
428 previously measured between sulfate and sulfide in the porewaters in 1991 (Fig. S2) and in
429 sediment incubations (Canfield et al., 2010). It is most evident from the oldest profile (Fig. S2)
430 that $\delta^{34}\text{S}$ sulfate and CRS values become progressively heavier with depth across the top 20 cm
431 typical of a closed system sulfate reduction. In fact, sedimentation rates of 2-4 mm/yr have been
432 reported for Lake Cadagno (Birch et al., 1996) which are rather high for a lake (Fiskal et al.,
433 2019).

434 Although CRS is on average more depleted in $\delta^{34}\text{S}$ in the deep glacial sediments than in
435 surface sediments, the difference between porewater sulfate and CRS is around the same as in
436 surface sediments (45.8‰). An gradient of progressively heavier CRS can be observed moving
437 upward through the sediment column away from the groundwater source. This suggests that
438 closed-system sulfate reduction is leading to similar $\delta^{34}\text{S}$ fractionations as in surface sediments.
439 What explains the rather light sulfate (+6.8 ‰) present in this deep layer remains unclear, but
440 oxidation of buried CRS by a groundwater source of oxidants offers a potential explanation.



441 In contrast, the relatively stable $\delta^{34}\text{S}$ isotopic signature of HAS (except one outlier value of
442 -25.9 ‰) over depth suggests that humic acid-bound sulfur is overwhelmingly formed in
443 surface sediments and not prone to significant alteration after formation and burial. This implies
444 that humic acid-bound S is extremely resistant to chemical or microbial transformation.

445 CONCLUSION

446 Here we report the first biogeochemical and isotopic data on sulfur cycling in ancient (up
447 to 13.5 kya) lake sediments. In addition to confirming the rapid sulfurization of organic matter,
448 we have documented two separate zones of CRS formation within the same sediment column,
449 the deeper one driven by sulfate-rich, oxidizing groundwater. Surprising similarities in S-
450 isotope fractionation patterns in surface and deep sediments are likely determined by closed
451 system S-isotope fractionation despite the very different sources of organic matter, sulfate
452 concentrations, and sulfur-cycling microbial communities. In other environments, sulfate
453 diffusing from aquifers (Fichtel et al., 2012) or evaporated sea water trapped in the sediments
454 (Vengosh et al., 1994) could essentially form new CRS with authigenic $\delta^{34}\text{S}$ signatures
455 potentially different from surface sediments. This phenomenon might actually be widespread
456 as submarine groundwater seepage is a common, understudied phenomenon and the basaltic
457 ocean crust is the largest aquifer system on Earth.

458 Deep sulfur cycling in Lake Cadagno appears to be driven by a diverse, and uncultivated
459 biosphere, as most *dsrB* lineages recovered here belong to novel taxa whose role in sulfur and
460 carbon cycling has yet to be revealed. These microorganisms, such as Chloroflexota, are not
461 classical sulfate-reducing bacteria that have been characterized thus far in the laboratory and
462 much is yet to be understood about their metabolisms. Nonetheless, the recovery of sulfur
463 oxidation genes (*soxB*) from presumably anoxic surface sediments and sulfate reduction genes



464 (*dsrB*) from sulfate-depleted deep sediments opens new questions about deep sources of
465 oxidants which could drive continued sulfur-cycling in such reducing environments.

466 **ACKNOWLEDGEMENTS**

467 We thank the entire 2019 Cadagno sampling crew for assistance in the field, and especially the
468 Alpine Biology Center Foundation (Switzerland) for use of its research facilities. We also
469 acknowledge Iso Christl, Rachele Ossola, and Jorge Spangenberg for their support with
470 chemical analyses. Longhui Deng. was sponsored by the Shanghai Pujiang Program
471 (22PJ1404800). This study was supported by the Swiss National Science Foundation (SNF)
472 grant No. 182096 (M.A.L.).

473 **COMPETING INTERESTS**

474 At least one author is a member of the editorial board of *Biogeosciences*.

475 **DATA AVAILABILITY**

476 *dsrB* gene sequences have been deposited in the NCBI database under Bioproject number
477 PRJNA991470. All other raw data has been deposited in SWISSUbase under study number
478 20541.

479 **4. AUTHOR CONTRIBUTIONS**

480 JSB performed sediment sampling and chemical analyses, synthesized the data and wrote the
481 manuscript. PCR and LD performed microbial community analyses and interpretations under
482 supervision of CM. SB provided S-isotope data from 1991 and 2019. HV and MM performed
483 sediment sampling and sedimentological characterizations and dating. MAL supervised this project.

484 **REFERENCES**

485 Amrani A. and Aizenshtat Z. (2004) Mechanisms of sulfur introduction chemically controlled: 834S
486 imprint. *Organic Geochemistry* **35**, 1319–1336.



- 487 Anantharaman K., Hausmann B., Jungbluth S. P., Kantor R. S., Lavy A., Warren L. A., Rappé M. S.,
488 Pester M., Loy A., Thomas B. C. and Banfield J. F. (2018) Expanded diversity of microbial
489 groups that shape the dissimilatory sulfur cycle. *ISME J* **12**, 1715–1728.
- 490 Anderson T. F. and Pratt L. M. (1995) Isotopic Evidence for the Origin of Organic Sulfur and Elemental
491 Sulfur in Marine Sediments. In *Geochemical Transformations of Sedimentary Sulfur* ACS
492 Symposium Series. American Chemical Society. pp. 378–396.
- 493 Baloza M., Henkel S., Geibert W., Kasten S. and Holtappels M. (2022) Benthic Carbon
494 Remineralization and Iron Cycling in Relation to Sea Ice Cover Along the Eastern Continental
495 Shelf of the Antarctic Peninsula. *Journal of Geophysical Research: Oceans* **127**,
496 e2021JC018401.
- 497 Berg J. S., Lepine M., Laymand E., Han X., Vogel H., Morlock M. A., Gajendra N., Gilli A., Bernasconi S.
498 M., Schubert C. J., Su G. and Lever M. A. (2022) Ancient and Modern Geochemical Signatures
499 in the 13,500-Year Sedimentary Record of Lake Cadagno. *Frontiers in Earth Science* **9**.
- 500 Bernasconi S. M., Meier I., Wohlwend S., Brack P., Hochuli P. A., Bläsi H., Wortmann U. G. and
501 Ramseyer K. (2017) An evaporite-based high-resolution sulfur isotope record of Late Permian
502 and Triassic seawater sulfate. *Geochimica et Cosmochimica Acta* **204**, 331–349.
- 503 Birch L., Hanselmann K. W. and Bachofen R. (1996) Heavy metal conservation in Lake Cadagno
504 sediments: Historical records of anthropogenic emissions in a meromictic alpine lake. *Water*
505 *Research* **30**, 679–687.
- 506 Bowles M. W., Mogollón J. M., Kasten S., Zabel M. and Hinrichs K.-U. (2014) Global rates of marine
507 sulfate reduction and implications for sub-sea-floor metabolic activities. *Science* **344**, 889–
508 891.
- 509 Bradley A. S., Leavitt W. D., Schmidt M., Knoll A. H., Girguis P. R. and Johnston D. T. (2016) Patterns of
510 sulfur isotope fractionation during microbial sulfate reduction. *Geobiology* **14**, 91–101.
- 511 Brunner B., Arnold G. L., Røy H., Müller I. A. and Jørgensen B. B. (2016) Off Limits: Sulfate below the
512 Sulfate-Methane Transition. *Front. Earth Sci.* **4**.
- 513 Brunner B. and Bernasconi S. M. (2005a) A revised isotope fractionation model for dissimilatory
514 sulfate reduction in sulfate reducing bacteria. *Geochimica et Cosmochimica Acta* **69**, 4759–
515 4771.
- 516 Brunner B. and Bernasconi S. M. (2005b) A revised isotope fractionation model for dissimilatory
517 sulfate reduction in sulfate reducing bacteria. *Geochimica et Cosmochimica Acta* **69**, 4759–
518 4771.
- 519 Bryant R. N., Houghton J. L., Jones C., Pasquier V., Halevy I. and Fike D. A. (2023) Deconvolving
520 microbial and environmental controls on marine sedimentary pyrite sulfur isotope ratios.
521 *Science* **382**, 912–915.
- 522 Canfield D. E., Farquhar J. and Zerkle A. L. (2010) High isotope fractionations during sulfate reduction
523 in a low-sulfate euxinic ocean analog. *Geology* **38**, 415–418.
- 524 Canfield D. E. and Thamdrup B. (1994) The Production of 34S-Depleted Sulfide During Bacterial
525 Disproportionation of Elemental Sulfur. *Science* **266**, 1973–1975.



- 526 Cypionka H., Smock A. M. and Böttcher M. E. (1998) A combined pathway of sulfur compound
527 disproportionation in *Desulfovibrio desulfuricans*. *FEMS Microbiology Letters* **166**, 181–186.
- 528 Damsté J. S. and De Leeuw J. W. (1990) Analysis, structure and geochemical significance of
529 organically-bound sulphur in the geosphere: State of the art and future research. *Organic*
530 *Geochemistry* **16**, 1077–1101.
- 531 Damsté J. S., Kok M. D., Köster J. and Schouten S. (1998) Sulfurized carbohydrates: an important
532 sedimentary sink for organic carbon? *Earth and Planetary Science Letters* **164**, 7–13.
- 533 David M. B. and Mitchell M. J. (1985) Sulfur constituents and cycling in waters, seston, and sediments
534 of an oligotrophic lake. *Limnology and Oceanography* **30**, 1196–1207.
- 535 Deng L., Meile C., Fiskal A., Bölsterli D., Han X., Gajendra N., Dubois N., Bernasconi S. M. and Lever M.
536 A. (2022) Deposit-feeding worms control subsurface ecosystem functioning in intertidal
537 sediment with strong physical forcing. *PNAS Nexus* **1**, pgac146.
- 538 Detmers J., Brüchert V., Habicht K. S. and Kuever J. (2001) Diversity of Sulfur Isotope Fractionations
539 by Sulfate-Reducing Prokaryotes. *Appl. Environ. Microbiol.* **67**, 888–894.
- 540 Ferdelman T. G., Church T. M. and Luther G. W. (1991) Sulfur enrichment of humic substances in a
541 Delaware salt marsh sediment core. *Geochimica et Cosmochimica Acta* **55**, 979–988.
- 542 Fichtel K., Mathes F., Könneke M., Cypionka H. and Engelen B. (2012) Isolation of Sulfate-Reducing
543 Bacteria from Sediments Above the Deep-Subseafloor Aquifer. *Front. Microbiol.* **3**.
- 544 Fike D. A., Bradley A. S. and Rose C. V. (2015) Rethinking the Ancient Sulfur Cycle. *Annual Review of*
545 *Earth and Planetary Sciences* **43**, 593–622.
- 546 Fiskal A., Deng L., Michel A., Eickenbusch P., Han X., Lagostina L., Zhu R., Sander M., Schroth M. H.,
547 Bernasconi S. M., Dubois N. and Lever M. A. (2019) Effects of eutrophication on sedimentary
548 organic carbon cycling in five temperate lakes. *Biogeosciences* **16**, 3725–3746.
- 549 Fossing H. and Jørgensen B. B. (1989) Measurement of bacterial sulfate reduction in sediments:
550 Evaluation of a single-step chromium reduction method. *Biogeochemistry* **8**, 205–222.
- 551 Gajendra N., Berg J. S., Vogel H., Deng L., Wolf S. M., Bernasconi S. M., Dubois N., Schubert C. J. and
552 Lever M. A. (2023) Carbohydrate compositional trends throughout Holocene sediments of an
553 alpine lake (Lake Cadagno). *Front. Earth Sci.* **11**, 1047224.
- 554 Goldhaber M. B. and Kaplan I. R. (1980) Mechanisms of sulfur incorporation and isotope fractionation
555 during early diagenesis in sediments of the gulf of California. *Marine Chemistry* **9**, 95–143.
- 556 Habicht K. S. and Canfield D. E. (1997) Sulfur isotope fractionation during bacterial sulfate reduction
557 in organic-rich sediments. *Geochimica et Cosmochimica Acta* **61**, 5351–5361.
- 558 Hashimoto Y., Shimamura S., Tame A., Sawayama S., Miyazaki J., Takai K. and Nakagawa S. (2022)
559 Physiological and comparative proteomic characterization of *Desulfolithobacter*
560 *dissulfuricans* gen. nov., sp. nov., a novel mesophilic, sulfur-disproportionating
561 chemolithoautotroph from a deep-sea hydrothermal vent. *Front. Microbiol.* **13**.



- 562 Hebbing Y., Schaeffer P., Behrens A., Adam P., Schmitt G., Schneckenburger P., Bernasconi S. M. and
563 Albrecht P. (2006) Biomarker Evidence for a Major Preservation Pathway of Sedimentary
564 Organic Carbon. *Science* **312**, 1627–1631.
- 565 Holmkvist L., Kamyshny A., Vogt C., Vamvakopoulos K., Ferdelman T. G. and Jørgensen B. B. (2011)
566 Sulfate reduction below the sulfate–methane transition in Black Sea sediments. *Deep Sea*
567 *Research Part I: Oceanographic Research Papers* **58**, 493–504.
- 568 Jochum L. M., Chen X., Lever M. A., Loy A., Jørgensen B. B., Schramm A. and Kjeldsen K. U. (2017)
569 Depth Distribution and Assembly of Sulfate-Reducing Microbial Communities in Marine
570 Sediments of Aarhus Bay. *Appl. Environ. Microbiol.* **83**.
- 571 Jørgensen B. B. (1982) Mineralization of organic matter in the sea bed—the role of sulphate
572 reduction. *Nature* **296**, 643–645.
- 573 Kallmeyer J., Ferdelman T. G., Weber A., Fossing H. and Jørgensen B. B. (2004) A cold chromium
574 distillation procedure for radiolabeled sulfide applied to sulfate reduction measurements.
575 *Limnology and Oceanography: Methods* **2**, 171–180.
- 576 Klein M., Friedrich M., Roger A. J., Hugenholtz P., Fishbain S., Abicht H., Blackall L. L., Stahl D. A. and
577 Wagner M. (2001) Multiple Lateral Transfers of Dissimilatory Sulfite Reductase Genes
578 between Major Lineages of Sulfate-Reducing Prokaryotes. *Journal of Bacteriology* **183**, 6028–
579 6035.
- 580 Kok M. D., Schouten S. and Sinninghe Damsté J. S. (2000) Formation of insoluble, nonhydrolyzable,
581 sulfur-rich macromolecules via incorporation of inorganic sulfur species into algal
582 carbohydrates. *Geochimica et Cosmochimica Acta* **64**, 2689–2699.
- 583 Lever M. A., Rouxel O., Alt J. C., Shimizu N., Ono S., Coggon R. M., Shanks W. C., Lapham L., Elvert M.,
584 Prieto-Mollar X., Hinrichs K.-U., Inagaki F. and Teske A. (2013) Evidence for Microbial Carbon
585 and Sulfur Cycling in Deeply Buried Ridge Flank Basalt. *Science* **339**, 1305–1308.
- 586 Lever M. A., Torti A., Eickenbusch P., Michaud A. B., Šantl-Temkiv T. and Jørgensen B. B. (2015) A
587 modular method for the extraction of DNA and RNA, and the separation of DNA pools from
588 diverse environmental sample types. *Front. Microbiol.* **6**.
- 589 Liu R., Wei X., Song W., Wang L., Cao J., Wu J., Thomas T., Jin T., Wang Z., Wei W., Wei Y., Zhai H., Yao
590 C., Shen Z., Du J. and Fang J. (2022) Novel Chloroflexi genomes from the deepest ocean
591 reveal metabolic strategies for the adaptation to deep-sea habitats. *Microbiome* **10**, 75.
- 592 Luther G. W. (1991) Pyrite synthesis via polysulfide compounds. *Geochimica et Cosmochimica Acta*
593 **55**, 2839–2849.
- 594 Mehrshad M., Rodriguez-Valera F., Amoozegar M. A., López-García P. and Ghai R. (2018) The
595 enigmatic SAR202 cluster up close: shedding light on a globally distributed dark ocean
596 lineage involved in sulfur cycling. *ISME J* **12**, 655–668.
- 597 Meyer B., Imhoff J. F. and Kuever J. (2007) Molecular analysis of the distribution and phylogeny of
598 the soxB gene among sulfur-oxidizing bacteria – evolution of the Sox sulfur oxidation enzyme
599 system. *Environmental Microbiology* **9**, 2957–2977.
- 600 Mitchell M. J., Landers D. H. and Brodowski D. F. (1981) Sulfur constituents of sediments and their
601 relationship to lake acidification. *Water Air Soil Pollut* **16**, 351–359.



- 602 Müller A. L., Kjeldsen K. U., Rattei T., Pester M. and Loy A. (2015) Phylogenetic and environmental
603 diversity of DsrAB-type dissimilatory (bi)sulfite reductases. *The ISME Journal* **9**, 1152–1165.
- 604 Nriagu J. O. and Soon Y. K. (1985) Distribution and isotopic composition of sulfur in lake sediments of
605 northern Ontario. *Geochimica et Cosmochimica Acta* **49**, 823–834.
- 606 Ono S., Sim M. S. and Bosak T. (2014) Predictive isotope model connects microbes in culture and
607 nature. *Proceedings of the National Academy of Sciences* **111**, 18102–18103.
- 608 Orr W. L. and Damsté J. S. (1990) Geochemistry of Sulfur in Petroleum Systems. In *Geochemistry of*
609 *Sulfur in Fossil Fuels* ACS Symposium Series. American Chemical Society. pp. 2–29.
- 610 Pellerin A., Antler G., Røy H., Findlay A., Beulig F., Scholze C., Turchyn A. V. and Jørgensen B. B.
611 (2018a) The sulfur cycle below the sulfate-methane transition of marine sediments.
612 *Geochimica et Cosmochimica Acta* **239**, 74–89.
- 613 Pellerin A., Antler G., Røy H., Findlay A., Beulig F., Scholze C., Turchyn A. V. and Jørgensen B. B.
614 (2018b) The sulfur cycle below the sulfate-methane transition of marine sediments.
615 *Geochimica et Cosmochimica Acta* **239**, 74–89.
- 616 Pester M., Knorr K.-H., Friedrich M. W., Wagner M. and Loy A. (2012) Sulfate-reducing
617 microorganisms in wetlands – fameless actors in carbon cycling and climate change. *Front.*
618 *Microbiol.* **3**.
- 619 Raven M. R., Adkins J. F., Werne J. P., Lyons T. W. and Sessions A. L. (2015) Sulfur isotopic
620 composition of individual organic compounds from Cariaco Basin sediments. *Organic*
621 *Geochemistry* **80**, 53–59.
- 622 Raven M. R., Crockford P. W., Hodgskiss M. S. W., Lyons T. W., Tino C. J. and Webb S. M. (2023)
623 Organic matter sulfurization and organic carbon burial in the Mesoproterozoic. *Geochimica*
624 *et Cosmochimica Acta* **347**, 102–115.
- 625 Raven M. R., Sessions A. L., Fischer W. W. and Adkins J. F. (2016) Sedimentary pyrite $\delta^{34}\text{S}$ differs
626 from porewater sulfide in Santa Barbara Basin: Proposed role of organic sulfur. *Geochimica*
627 *et Cosmochimica Acta* **186**, 120–134.
- 628 Rudd J. W. M., Kelly C. A. and Furutani A. (1986) The role of sulfate reduction in long term
629 accumulation of organic and inorganic sulfur in lake sediments1. *Limnology and*
630 *Oceanography* **31**, 1281–1291.
- 631 Schubert C. J., Vazquez F., Lösekann-Behrens T., Knittel K., Tonolla M. and Boetius A. (2011) Evidence
632 for anaerobic oxidation of methane in sediments of a freshwater system (Lago di Cadagno).
633 *FEMS Microbiology Ecology* **76**, 26–38.
- 634 Sim M. S., Bosak T. and Ono S. (2011) Large Sulfur Isotope Fractionation Does Not Require
635 Disproportionation. *Science* **333**, 74–77.
- 636 Slobodkin A. I. and Slobodkina G. B. (2019) Diversity of Sulfur-Disproportionating Microorganisms.
637 *Microbiology* **88**, 509–522.
- 638 Steingruber S. M., Bernasconi S. M. and Valenti G. (2020) Climate Change-Induced Changes in the
639 Chemistry of a High-Altitude Mountain Lake in the Central Alps. *Aquat Geochem.*



- 640 Treude T., Krause S., Maltby J., Dale A. W., Coffin R. and Hamdan L. J. (2014) Sulfate reduction and
641 methane oxidation activity below the sulfate-methane transition zone in Alaskan Beaufort
642 Sea continental margin sediments: Implications for deep sulfur cycling. *Geochimica et*
643 *Cosmochimica Acta* **144**, 217–237.
- 644 Urban N. R., Ernst K. and Bernasconi S. (1999) Addition of sulfur to organic matter during early
645 diagenesis of lake sediments. *Geochimica et Cosmochimica Acta* **63**, 837–853.
- 646 Vengosh A., Starinsky A. and Anati D. A. (1994) The origin of Mediterranean interstitial waters—relics
647 of ancient Miocene brines: A re-evaluation. *Earth and Planetary Science Letters* **121**, 613–
648 627.
- 649 Vuillemin A., Kerrigan Z., D’Hondt S. and Orsi W. D. (2020) Exploring the abundance, metabolic
650 potential and gene expression of subseafloor Chloroflexi in million-year-old oxic and anoxic
651 abyssal clay. *FEMS Microbiology Ecology* **96**, fiae223.
- 652 Wasmund K., Mußmann M. and Loy A. (2017) The life sulfuric: microbial ecology of sulfur cycling in
653 marine sediments. *Environmental Microbiology Reports* **9**, 323–344.
- 654 Wasmund K., Schreiber L., Lloyd K. G., Petersen D. G., Schramm A., Stepanauskas R., Jørgensen B. B.
655 and Adrian L. (2014) Genome sequencing of a single cell of the widely distributed marine
656 subsurface Dehalococcoidia, phylum Chloroflexi. *ISME J* **8**, 383–397.
- 657 Werne J. P., Lyons T. W., Hollander D. J., Formolo M. J. and Sinninghe Damsté J. S. (2003) Reduced
658 sulfur in euxinic sediments of the Cariaco Basin: sulfur isotope constraints on organic sulfur
659 formation. *Chemical Geology* **195**, 159–179.
- 660 Wirth S. B., Gilli A., Niemann H., Dahl T. W., Ravasi D., Sax N., Hamann Y., Peduzzi R., Peduzzi S.,
661 Tonolla M., Lehmann M. F. and Anselmetti F. S. (2013) Combining sedimentological, trace
662 metal (Mn, Mo) and molecular evidence for reconstructing past water-column redox
663 conditions: The example of meromictic Lake Cadagno (Swiss Alps). *Geochimica et*
664 *Cosmochimica Acta* **120**, 220–238.
- 665 Wortmann U. G., Bernasconi S. M. and Böttcher M. E. (2001) Hypersulfidic deep biosphere indicates
666 extreme sulfur isotope fractionation during single-step microbial sulfate reduction. *Geology*
667 **29**, 647–650.
- 668